Journal of Assisted Reproduction and Genetics (2019) 36:1195–1210
https://doi.org/10.1007/s10815-019-01447-4

REPRODUCTIVE PHYSIOLOGY AND DISEASE

Gene expression analysis of follicular cells revealed inflammation as a potential IVF failure cause

Chloé S. Fortin[1] · Arthur Leader[2] · Neal Mahutte[3] · Scot Hamilton[4] · Marie-Claude Léveillé[2] · Marc Villeneuve[5] · Marc-André Sirard[1]

Received: 15 October 2018 / Accepted: 29 March 2019 / Published online: 18 April 2019

Abstract

Purpose Hormonal stimulation prior to IVF influences the ovarian environment and therefore impacts oocytes and subsequent embryo quality. Not every patient has the same response to the same treatment and many fail for unknown reasons. Knowing why a cycle has failed and how the follicles were affected would allow clinicians to adapt the treatment accordingly and improve success rate. This study examines the hypothesis that transcriptomic analysis of follicular cells from failed IVF cycles reveals potential reasons for failure and provides new information on the physiological mechanisms related to IVF failure.

Methods Follicular cells (granulosa cells) were obtained from IVF patients of four Canadian fertility clinics. Using microarray analysis, patients that did not become pregnant following the IVF cycle were compared to those that did. Functional analysis was performed using ingenuity pathway analysis and qRT-PCR was used to validate the microarray results in a larger cohort of patients.

Results The microarray showed 165 differentially expressed genes (DEGs) in the negative group compared to the pregnancy group. DEGs include many pro-inflammatory cytokines and other factors related to inflammation, suggesting that this process might be altered when IVF fails. Overexpression of several factors, some of which act upstream from vascular endothelial growth factor (VEGF), also indicates increased permeability and vasodilation. Some DEGs were related to abnormal differentiation and increased apoptosis.

Conclusions Our results suggest that failure to conceive following IVF cycles could be associated with an imbalance between pro-inflammatory and anti-inflammatory mediators. The findings of this study identify potential failure causes and pathways for further investigation. Stimulatory protocols personalized according to patient response could improve the chances of later success.

Keywords Follicular cells · Gene expression · Granulosa cells · Inflammation · In vitro fertilization · Microarray

Electronic supplementary material The online version of this article (https://doi.org/10.1007/s10815-019-01447-4) contains supplementary material, which is available to authorized users.

✉ Marc-André Sirard
Marc-Andre.Sirard@fsaa.ulaval.ca

[1] Centre de recherche en reproduction, développement et santé intergénérationnelle (CRDSI), Université Laval, 2440 Boulevard Hochelaga, Québec, QC G1V 0A6, Canada

[2] Ottawa Fertility Centre, 100-955 Green Valley Crescent, Ottawa, ON K2C 3V4, Canada

[3] Montréal Fertility Centre, 5252 de Maisonneuve Boulevard West Suite 220, Montréal, QC H4A 3S5, Canada

[4] Reproductive Care Centre, 2180 Meadowvale Boulevard, Toronto, ON L5N 5S3, Canada

[5] PROCREA Cliniques, 5600 Boulevard des Galeries, Québec, QC G2K 2H6, Canada

Introduction

Since the last decades, the incidence of human infertility has increased worldwide. Infertile couples wishing to build their family are turning more often to assisted reproductive technologies such as in vitro fertilization with embryo transfer (IVF-ET). While remarkable progress has been made since the introduction of this procedure almost 30 years ago, the success rate remains low, with two out of three IVF cycles failing to lead to pregnancy [1, 2]. Considering the emotional burden and high costs of this procedure, this is a real concern for patients and society. The improvement of the success rate remains a priority and understanding why a given cycle has failed is certainly one of the key factors.

Ovarian stimulation prior to IVF influences the ovarian environment and therefore oocyte and subsequent embryo

quality. The follicular cells and the oocyte form a functional unit and their proper development depends strongly on a complex bidirectional communication system involving paracrine and autocrine factors [3, 4]. Since follicular cells reflect oocyte quality, gene expression has been extensively studied in these cells to identify predictive non-invasive biomarkers of oocyte and embryo competence. Changes in gene expression were correlated with various success parameters in granulosa cells [5–8] and with pregnancy [9–12] and oocyte or embryo competence [13–16] in cumulus cells. These numerous studies analyzing the transcriptomic profile of follicular cells therefore focused on finding biomarkers predictive of IVF success. These all aimed to provide novel and non-invasive selection tools to choose oocytes or embryos with the highest chance of pregnancy. Surprisingly, few studies have focused on determining what could have gone wrong in failed IVF cycles. This information would help physicians to better assess the impact of the stimulation protocols, including the induction timing, in order to potentially improve the next stimulation cycles and directly generate better oocytes and embryos.

In the light of this information, we hypothesize that follicular cell's gene expression is different in failed IVF patients compared to those who successfully get pregnant after IVF. By analyzing the RNA content of granulosa cells aspirated with the oocyte, it would be possible to identify the global follicular picture resulting from ovarian stimulation. We believe that a pool of granulosa cells from follicles of a given cycle can provide information on what went wrong and could later provide useful biomarkers associated with the cause of failure. Therefore, the aim of this study was to determine how gene expression is affected in follicles from failed IVF cycles and how the differential gene expression can inform on the cause of pregnancy failure. This information could be helpful in guiding physicians for their next IVF cycle, leading to an improved stimulation protocol according to the individual patient's response.

Materials and methods

Patients and follicular cell recovery

Follicular cells composed principally of granulosa cells were obtained from consenting patients registered at the Ottawa Fertility Center (Ottawa, ON, Canada), the Reproductive Care Center (Toronto, ON, Canada), the Montréal Fertility Center (Montréal, QC, Canada), or Cliniques PROCREA (Québec, QC, Canada). All women received a hormonal treatment to stimulate follicular growth for IVF procedure. Patients with polycystic ovary syndrome (PCOS), who were 43 years or older, whose partner had severe male factor infertility or who received a modified natural cycle treatment were not included in the study.

Samples were collected irrespective of the hormonal protocol used. Follicular fluid, follicular cells, and oocytes were collected by ultrasound-guided aspiration 34 to 36 h after the ovulation trigger was administered. The oocytes and surrounding cumulus cells were removed for the IVF or ICSI procedure. To isolate follicular cells, containing mural granulosa cells, follicular fluids from all the follicles aspirated from the same patient were pooled into a single sample, which was then centrifuged at room temperature for 10 min at 800×*g*. The resulting pellet was suspended in 500 μL of phosphate-buffered saline solution at 4 °C and transferred to a cryovial. After centrifugation at 2000×*g* for 1 min (room temperature), the supernatant was removed and cells were frozen quickly in liquid nitrogen. Embryo development, embryo transfer, and treatment outcome information were collected. We are aware that our samples are probably not 100% pure isolated granulosa cells, but are rather principally composed of granulosa cells and might possibly contain contaminating blood-derived cells. However, the use of the term "granulosa cells" when referring to our sample is to avoid confusion with other follicular cell types like theca cells and cumulus cells.

RNA extraction

Total RNA was extracted from the samples using TRIzol® reagent (Invitrogen, Burlington, ON, Canada) following the manufacturer's protocol. The RNA was purified further using the ARCTURUS® PicoPure® RNA Isolation Kit protocol (Applied Biosystems, Burlington, ON, Canada) including the treatment with the RNase-free DNase Set (Qiagen) directly on the extraction column. RNA quality, purity, and concentration were analyzed using the Agilent Bioanalyzer 2100 (Agilent technologies Inc., Santa Clara, CA, USA) with the RNA 6000 Nano Kit (Agilent Technologies). Samples showing good quality RNA with an integrity number over 7.0 were kept for the study.

Treatment assignment

Based on patient pregnancy outcome, the samples were divided into positive and negative groups. The positive group included all patients for which pregnancy was confirmed by ultrasonographic visualization of heartbeat at 6–8 weeks of gestation. The negative group includes the samples associated to negative pregnancy outcome. For the negative patients, none of the embryos obtained after this IVF cycle led to a successful pregnancy. A patient was therefore assigned to the negative group only when all the embryos produced in the stimulation cycle were used, whether during fresh transfer or during subsequent frozen-thawed transfers.

Microarray gene expression analysis design

The microarray analysis was performed using 32 samples, 16 from negative (no pregnancy) group and 16 from positive (pregnancy) group. Each group of 16 samples contained four samples drawn randomly from each of the four clinics. The 16 samples were then divided into four pools each containing one sample from each clinic. Such pooling decreases the statistical noise due to individual variation and removes the potential effects of treatment variation across clinics. The four biological replicate pools from the negative group were compared to those of the positive group on a four-array slide in dye-swap.

RNA amplification, labeling, and microarray hybridization

In order to have enough material for the microarray experiment, the eight pools were amplified using the ARCTURUS® RiboAmp® PLUS RNA Amplification Kit (Applied Biosystems, Burlington, Canada) according to the manufacturer's instructions. The resulting amplified antisense RNA (aRNA) was quantified using a Nano-Drop ND-1000 device (NanoDrop Technologies, Wilmington, DE, USA). For each pool, 4 μg of aRNA was labeled with Cy3 or Cy5 using the ULS™ Fluorescent Labelling Kit for Agilent arrays (Kreatech Diagnostics, Amsterdam, Netherlands). The labeled product was then purified using the ARCTURUS® PicoPure® RNA Isolation Kit (Applied Biosystems, Burlington, ON, Canada). The Nano-Drop ND-1000 (NanoDrop Technologies, Wilmington, DE, USA) was used to measure the labeling efficiency. Finally, the samples were hybridized on the 4x44k V2 Whole human genome microarray (Agilent).

A total of 825 ng of each labeled sample (Cy3 and Cy5) was incubated in a solution containing 10× blocking agent and 25× fragmentation buffer in a volume of 55 μL at 60 °C for 15 min and then placed immediately on ice. HI-RPM hybridization buffer (Agilent) was added (55 μL of 2× GEx) for a total volume of 110 μL, and the mixture was loaded (100 μL) onto the array and hybridized at 65 °C for 17 h in an Agilent chamber in a rotating oven. Slides were then washed with gene expression wash buffer 1 (containing 0.005% Triton X-102) for 3 min at room temperature and then transferred to gene expression wash buffer 2 (also containing 0.005% Triton X-102) for 3 min at 42 °C. Final washes at room temperature with acetonitrile (for 10 s at room temperature) and with drying and stabilization solution (for 30 s at room temperature) were performed before air-drying the slides. The slides were scanned using the Tecan PowerScanner microarray scanner (Tecan Group Ltd., Männerdorf, Switzerland), and ArrayPro 6.4 (Media Cybernetics, Bethesda, MD, USA) was used to extract features [17].

Microarray data normalization and statistical analysis

Microarray data were processed using a procedure described by Nivet et al. [17] with FlexArray version 1.6.3 [18], a software package that uses R and BioConductor for statistical analysis of microarray gene expression data. They were corrected using a simple background subtraction and normalized using Loess within-array normalization and between-array quantile normalization. Statistical analysis was then performed using the Limma package provided in FlexArray. Differences between treatments were considered significant when the Limma *P* value was less than 0.05.

Ingenuity pathway analysis

The normalized data were also imported into the Ingenuity Pathway Analysis software (IPA, Ingenuity Systems, www.ingenuity.com). IPA integrates information from a large variety of experimental platforms. It is able to generate gene networks showing potential interactions between molecules and to perform a functional analysis of the associated biological functions and molecular processes. Ingenuity pathway analysis was used to obtain a biological interpretation of the combination of differentially expressed genes and thus explore what could be affected in the patients with failed IVF cycle. This software reveals metabolic relationships, mechanisms, functions, and pathways that may be related to changes in gene expression observed using microarray analysis. The analyses were carried out using cut-offs of 1.5 for the fold-change and 0.05 for the *P* value.

Preparation of cDNA and quantitative RT-PCR validation

Quantitative RT-PCR (qRT-PCR) was used to validate the microarray results. The qRT-PCR was performed with two technical replicates per patient. The validation was done on the 32 patients of the array but also on an enlarged cohort of 97 patients. For each sample, 1000 ng of RNA was reverse-transcribed using the qScript™ Flex cDNA Synthesis Kit (Quanta BioSciences Inc., Gaithersburg, MD, USA) with oligo dT primers according to manufacturer's specifications.

Six genes among the most differentially expressed in terms of fold-change were analyzed by qRT-PCR, namely chemokine C-X-C motif ligand 2 (*CXCL2*), docking protein 5 (*DOK5*), interleukin 1 beta (*IL1B*), interleukin 8 (*IL8*), neurotensin (*NTS*), and prothymosin alpha (*PTMA*). Upstream regulator genes identified by IPA are not analyzed by qRT-PCR since their activation is determined by the genes they control downstream (observed in the array) and not by their actual level of expression at the time of oocyte recovery. In addition, to avoid the possibility that the transcriptomic data be skewed by differences in contaminating blood-derived

cells, we also analyzed the expression of leukocyte antigen *CD45* in all our samples.

Primers were designed using the Integrated DNA Technologies PrimerQuest tool (http://www.idtdna.com/primerquest) and tested using cDNA from a pooled sample. The primer sequences selected for each gene are presented in Supplementary Table S1. To ensure the specificity of the primers, amplified fragments were visualized on a standard 1.25% agarose gel, purified using a QIAquick® PCR Purification Kit (Qiagen) and sequenced. The purified PCR products were then quantified using the NanoDrop ND-1000 device and a standard curve was obtained using serial dilutions ranging from 2×10^{-3} to 2×10^{-8} ng/μL.

Quantitative RT-PCR was performed on a LightCycler 480 device (Roche Diagnostics, Laval, QC, Canada) using PerfeCTa® SYBR® Green SuperMix (Quanta BioSciences Inc., Gaithersburg, MD, USA) for real-time monitoring. Each reaction was performed in a final mixture volume of 20 μL containing 2 μL of cDNA, 0.25 μM of each primer, and 1× SYBR Green. The PCR conditions were the same for all genes, with initial denaturation at 95 °C for 10 min, 50 amplification cycles (denaturing at 95 °C for 10 s, annealing at 57 °C for 10 s, and extension at 72 °C for 20 s), followed by a melting curve (95 °C) and a final cooling step at 40 °C. Quantification was performed by comparison with the standard curve using LightCycler 480 software version 1.5 (Roche Diagnostics). Melting curve analysis provided by the LightCycler software was used to confirm PCR specificity.

Normalization and statistical analysis of quantitative RT-PCR results

Analysis of gene expression stability over the different samples was performed using the GeNorm VBA applet software as described by Vandesompele et al. [19]. Four reference genes were tested: actin beta (*ACTB*), glyceraldehyde 3-phosphate dehydrogenase (*GAPDH*), cyclophilin A (*PPIA*), and tyrosine 3-monooxygenase/tryptophan 5-monooxygenase activation protein zeta (*YWHAZ*). The most stable reference genes were identified by the stepwise exclusion of the least stable gene and recalculating the *M* values (internal control gene stability). Following GeNorm analysis, *GAPDH, PPIA*, and *YWHAZ* were designated as the most stable genes, with *M* values of less than 1.5, as recommended by the software developer. Quantitative RT-PCR data were thus normalized on these three reference genes. Statistical analyses were performed using GraphPad Prism 6 software (GraphPad Software Inc., La Jolla, CA, USA). The *t* test and Mann-Whitney test (if data did not reach normality criteria) were used to identify statistically significant differences ($P < 0.05$) in mRNA levels between the two groups. Results are presented as the mean ± standard error mean.

Results

Patient variables

Eight pools of follicular cells (four negative pools vs four positive pools) were included in the microarray gene expression contrast analysis. The demographic features and cycle parameters of the population used to make these pools are presented in Tables 1 and 2. The patients included in the study were not PCOS and no patient showed clinical ovarian hyperstimulation syndrome (OHSS) either. They were undergoing infertility treatment due to tubal factor, endometriosis, advanced maternal age, diminished ovarian reserved, unexplained infertility, or no male partner (Table 2). The simulation protocol was either antagonist or long agonist protocol and the proportion of patients receiving each protocol was similar in both groups. In positive group, five patients received a long agonist protocol and 11 received an antagonist protocol while in negative group, four patients received a long agonist protocol and 12 received an antagonist protocol. The patients received recombinant FSH alone or combined with recombinant LH or highly purified hMG. Patients were on average 34 years old (min 28, max 39) and most of them were at their first or second IVF cycle. Level of FSH on days 2 to 4 of the menstrual cycle was similar between the groups as well as the number of days of stimulation and the total dose of gonadotrophin used. There were no significant differences between the positive and negative groups regarding endometrial thickness around trigger, serum estradiol and number of follicles on the day of trigger or number of cumulus-oocyte complexes retrieved. The proportion of matured oocytes (metaphase II) was apparently higher among the patients of positive group, but not significantly. However, this could explain the higher fertilization rate found in the positive group ($P = 0.03$). The mean number of embryos per transfer tended to be higher in the negative group compared to the positive group, but this is probably caused by one patient having three embryos transferred, which is quite unusual.

Gene expression analysis

Differential expression (a change ≥ 1.5-fold and a *P* value ≤ 0.05) between cells from follicles associated with failed IVF cycles (negative) and successful IVF cycles (positive) was found for a total of 165 genes (Supplementary Table S2). Among these, 63 were significantly overexpressed (i.e., upregulated genes) and 102 were significantly under-expressed (i.e., downregulated genes) in the negative group compared to the positive group (data not shown). The top 20 upregulated and downregulated genes in the negative group are shown in Table 3.

Table 1 Demographic features and cycle parameters in both groups

Parameter	Positive group			Negative group			*P* value
	n	Mean	SD	*n*	Mean	SD	
Age	16	34.44	3.18	16	34.50	3.06	0.768
Prior cycles	16	0.75	1.13	16	0.63	0.96	0.917
Days of stimulation	16	9.38	1.20	16	9.69	2.12	0.929
Total IU FSH used (IU)	16	2582.84	933.68	16	2540.63	1220.96	0.484
FSH days 2 to 4 (IU/ml)[a]	12	6.94	2.13	16	5.83	2.11	0.177
E2 on the day of trigger (pmol/l)[a]	12	6982.08	3172.11	13	6562.77	4239.85	0.461
Endometrial thickness (mm)[a]	12	11.17	2.53	13	10.84	1.83	0.936
No. of follicles on day of trigger	16	14.25	10.94	16	13.25	5.57	0.830
No. of COC retrieved	16	9.38	5.02	16	9.69	2.60	0.530
Oocyte maturity (%)[a]	14	82%	18%	15	72%	15%	0.064
Fertilization rate (%)	16	73%	19%	16	59%	27%	0.029*
No. of embryos per transfer	16	1.25	0.45	16	1.69	0.60	0.056

Prior cycles = number or prior IVF cycles for the patient, endometrial thickness = thickness of endometrium within a few days of trigger, oocyte maturity = no. of MII oocytes/no. of COC retrieved, fertilization rate = no. of 2PN/no. of COC used for fertilization

[a] Some data are missing for these parameters because they were not routinely measured on all patients of the clinic

*Fertilization rate was significantly lower in the negative group ($P < 0.05$) compared to the positive group following Mann-Whitney *t* test

Pathway analysis

Ingenuity pathway analysis was used to obtain a biological interpretation of the combination of differentially expressed genes and thus explore what could be affected in the patients with failed IVF cycle. This software reveals metabolic relationships, mechanisms, functions, and pathways that may be related to changes in gene expression observed using microarray analysis.

The biological functions significantly affected in the negative patients were identified following functional analysis of the differentially expressed genes. The functions most affected are shown in Table 4. These include two biological functions related to immune response, namely immune cell trafficking and inflammatory response. These are top categories and regroup several sub-functions. Table 5 shows that nearly all the significant underlying sub-functions are related to inflammation. Taking into account how the direction of change of the genes matches with the activation state of a function, IPA calculates an activation score (*z* score). The *z* score, depending if it is positive or negative, predicts that the biological process is trending towards an increase or a decrease. A *z* score above 2.0 or below − 2.0 is considered significantly predictive, which means that the trend is highly statistically significant. In the present analysis, all the significant sub-functions except one showed positive *z* scores (2.00–3.11), thus predicting an increase in these processes. With a *z* score of − 2.63, apoptosis of leukocytes is the only function predicted to decrease. We can also see that there is considerable overlap between the top functions, with many sharing the same sub-functions. The most redundant are recruitment of neutrophils, phagocytes,

Table 2 Distribution of stimulation protocol parameters between patients of both groups

Parameters	Positive group (*n*)	Negative group (*n*)
Age	16	16
Below 30	0	1
30–35	11	10
Over 35	5	5
Infertility diagnosis	16	16
Advanced maternal age	2	0
Diminished ovarian reserve	1	2
Endometriosis	5	3
Unexplained	5	5
No male partner	1	2
Tubal	2	4
Protocol	16	16
Antagonist	11	12
Long agonist	5	4
Days of stimulation	16	16
7–8 days	5	6
9–10 days	7	6
11–13 days	4	4
Total IU FSH used (IU)	16	16
Below 2500	11	10
2500–5000	5	6

Table 3 Top 20 up-regulated and down-regulated genes in granulosa cells from follicles associated with failure of IVF in comparison with those associated with success

Up-regulated genes				Down-regulated genes			
Gene symbol	Description	Relative change	P value	Gene symbol	Description	Relative change	P value
UMODL1	uromodulin like 1	2.471	5.55E-03	*PTMA*	prothymosin, alpha	-2.326	5.42E-04
AQP2	aquaporin 2	2.278	1.67E-02	*BBX*	bobby sox homolog (*Drosophila*)	-2.239	4.46E-03
DPY19L2P1	DPY19L2 pseudogene 1	2.194	7.68E-03	*IL6ST*	interleukin 6 signal transducer	-2.200	1.72E-02
DPYSL4	dihydropyrimidinase like 4	2.161	3.48E-02	*ARGLU1*	arginine and glutamate rich 1	-2.121	1.42E-02
CCL3	chemokine (C-C motif) ligand 3	2.074	2.41E-02	*HIST1H4L*	histone cluster 1, H4l	-2.105	1.97E-02
CRNN	cornulin	2.057	2.11E-02	*TAOK1*	TAO kinase 1	-2.093	1.05E-03
MT3	metallothionein 3	2.030	1.85E-02	*SSB*	Sjogren syndrome antigen B	-2.053	1.13E-02
NTS	neurotensin	1.996	1.91E-02	*BRD3*	bromodomain containing 3	-2.036	2.75E-03
IL8	interleukin 8	1.984	1.73E-02	*SLC35E3*	solute carrier family 35 member E3	-2.013	1.09E-03
LOX	lysyl oxidase	1.979	5.32E-03	*ZCCHC17*	zinc finger, CCHC domain containing 17	-1.989	3.67E-02
CXCL2	chemokine (C-X-C motif) ligand 2	1.974	1.37E-02	*BCAS1*	breast carcinoma amplified sequence 1	-1.970	2.07E-02
CSMD3	CUB and Sushi multiple domains 3	1.954	8.48E-04	*HIST1H4B*	histone cluster 1, H4b	-1.919	9,98E-03
DOK5	docking protein 5	1.865	1.43E-02	*AR*	androgen receptor	-1.916	2,27E-03
LOC400548	uncharacterized LOC400548	1.855	2.14E-02	*LITAF*	lipopolysaccharide-induced TNF factor	-1.910	1.96E-02
C17orf109	small integral membrane protein 5	1.844	2.35E-02	*BAZ1B*	bromodomain adjacent to zinc finger domain 1B	-1.890	5.78E-03
IL1B	interleukin 1 beta	1.793	4.47E-02	*PSMD10*	proteasome 26S subunit, non-ATPase 10	-1.883	3.07E-03
GJA1	gap junction protein alpha 1	1.785	4.54E-02	*CHD9*	chromodomain helicase DNA binding protein 9	-1.877	6.73E-03
FLJ22447	uncharacterized LOC400221	1.777	4.07E-02	*CSNK1G2*	casein kinase 1, gamma 2	-1.863	3.32E-02
GULP1	GULP, engulfment adaptor PTB domain containing 1	1.769	4.56E-02	*PSCA*	prostate stem cell antigen	-1.861	2.86E-02
BEND5	BEN domain containing 5	1.766	2.11E-02	*HLA-DQB1*	major histocompatibility complex, class II, DQ beta 1	-1.859	7.78E-03

and monocytes, which are all involved in the same five functions.

IPA upstream analysis also predicted the activation of relevant upstream regulators based on the expression levels of their downstream targets to make possible the combination of several genes as an indicator of an activated function or pathway. Activation of these upstream regulators could have led to or contributed to the changes observed in this contrast. Analyzing these pathways might also help us determine in which way the oocytes were affected in the negative patients. Among the upstream regulators involved in ovarian functions, early growth response 1 (*EGR1*) and interleukin 1 beta (*IL1B*) are particularly interesting (Table 6). Indeed, these factors act upstream of many cytokines and inflammation-related genes (Fig. 1). In fact, many of the upstream regulators thus identified are related to inflammatory processes, such as interleukin 6 (*IL-6*), interleukin 17 (*IL-17*), selectin P ligand (*SELPLG*), interleukin 10 receptor subunit A (*IL-10RA*), and others.

Quantitative RT-PCR validation

Six genes found among the most differentially expressed in the microarray contrast (*CXCL2, DOK5, IL1B, IL8, NTS*, and

Table 4 The biological functions affected most significantly by the measured changes in gene expression patterns, from ingenuity pathway analysis

Biological function	*P* value
Cancer-related	1.82E−13–5.15E−03
Organismal injury and abnormalities	1.82E−13–5.15E−03
Hematological system development and function	5.51E−08–5.15E−03
Immune cell trafficking	5.51E−08–5.15E−03
Cellular movement	5.51E−08–5.15E−03
Inflammatory response	5.51E−08–5.15E−03
Tissue development	6.42E−08–4.53E−03
Skeletal and muscular system development and function	1.76E−07–5.15E−03
Cell-to-cell signaling and interaction	4.43E−07–4.81E−03
Cellular growth and proliferation	3.02E−06–5.15E−03
Cell death and survival	5.14E−06–5.15E−03
Cellular development	8.24E−06–4.74E−03
Organ development	8.24E−06–4.53E−03
Hematopoiesis	1.35E−05–4.62E−03
Cardiovascular system development and function	1.67E−05–5.15E−03

The *P* value is the probability that the association between the change in gene expression and the suggested biological function is due to chance. It is presented as a range since each function includes several sub-functions

Table 5 Significant sub-functions and predicted activation state associated with the biological functions most strongly suggested by changes in gene expression levels

Biological Function	Sub-function	Predicted activation	*z* score	Molecules
Hematological system dev. and function, inflammatory response	Quantity of phagocytes	Increased	3.11	12
Cellular movement	Homing of cells	Increased	2.91	14
Cellular movement	Chemotaxis of cells	Increased	2.62	12
Hematological system dev. and function, inflammatory response	Quantity of neutrophils	Increased	2.61	7
Cellular movement, hematological system dev. and function, immune cell trafficking, inflammatory response	Infiltration of phagocytes	Increased	2.60	8
Cell-mediated immune response, cellular movement, hematological system dev. and function, immune cell trafficking	Cell movement of T lymphocytes	Increased	2.58	8
Hematological system dev. and function, immune cell trafficking, inflammatory response, tissue dev.	Accumulation of myeloid cells	Increased	2.54	9
Cellular movement	Migration of blood cells	Increased	2.51	20
Cellular movement, hematological system dev. and function, immune cell trafficking	Infiltration of leukocytes	Increased	2.48	12
Cellular movement, hematological system dev. and function, immune cell trafficking	Infiltration by mononuclear leukocytes	Increased	2.41	7
Cellular movement, hematological system development and function	Mobilization of blood cells	Increased	2.41	6
Cellular movement, immune cell trafficking	Leukocyte migration	Increased	2.38	19
Inflammatory response	Degranulation of phagocytes	Increased	2.34	6
Cell-to-cell signaling and interaction, cellular movement, hematological system dev. and function, immune cell trafficking, inflammatory response	Recruitment of phagocytes	Increased	2.29	9
Cellular movement	Homing of blood cells	Increased	2.28	11
Cell-to-cell signaling and interaction, cellular movement, hematological system dev. and function, immune cell trafficking	Recruitment of leukocytes	Increased	2.28	10
Cancer-related, cellular dev., cellular growth and proliferation, organismal injury and abnormalities	Proliferation of tumor cells	Increased	2.26	12
Hematological system dev. and function	Quantity of blood	Increased	2.26	7
Cell-to-cell signaling and interaction	Adhesion of blood cells	Increased	2.25	10
Cellular movement, hematological system dev. and function, immune cell trafficking	Cell movement of antigen-presenting cells	Increased	2.24	12
Cellular movement, hematological system dev. and function, immune cell trafficking	Cell movement of myeloid cells	Increased	2.24	18
Cellular movement, hematological system dev. and function, immune cell trafficking, inflammatory response	Cell movement of macrophages	Increased	2.23	11
Cellular movement, hematological system dev. and function, immune cell trafficking, inflammatory response	Infiltration by neutrophils	Increased	2.23	9
Cellular movement, hematological system dev. and function, immune cell trafficking, inflammatory response	Cell movement of monocytes	Increased	2.23	8
Cellular movement, hematological system dev. and function, immune cell trafficking, inflammatory response	Influx of neutrophils	Increased	2.22	5
Cellular movement, hematological system dev. and function, immune cell trafficking, inflammatory response	Mobilization of neutrophils	Increased	2.22	5
Cellular movement, hematological system dev. and function, immune cell trafficking	Infiltration by lymphocytes	Increased	2.21	6
Cellular movement, hematological system dev. and function, immune cell trafficking	Cell movement of eosinophils	Increased	2.20	5
Cell-to-cell signaling and interaction, cellular movement, hematological system dev. and function, inflammatory response	Recruitment of monocytes	Increased	2.20	6
Cellular movement	Chemoattraction	Increased	2.20	5
Cellular movement, hematological system dev. and function, immune cell trafficking, inflammatory response	Infiltration of macrophages	Increased	2.19	6
Tissue development	Accumulation of cells	Increased	2.18	10
Cellular movement, hematological system dev. and function, immune cell trafficking, inflammatory response	Cell movement of phagocytes	Increased	2.16	18
Organ development	Dev. of lymphatic system component	Increased	2.15	8
	Chemotaxis of myeloid cells	Increased	2.15	9

Table 5 (continued)

Biological Function	Sub-function	Predicted activation	*z* score	Molecules
Cellular movement, hematological system dev. and function, immune cell trafficking, inflammatory response				
Cellular movement, hematological system dev. and function, immune cell trafficking	Homing of leukocytes	Increased	2.12	10
Cellular movement	Transmigration of blood cells	Increased	2.09	6
Cellular movement	Migration of cells	Increased	2.08	32
Cancer-related, organismal injury and abnormalities	Cancer	Increased	2.04	143
Cell-to-cell signaling and interaction, cellular movement, hematological system dev. and function, immune cell trafficking, inflammatory response	Recruitment of neutrophils	Increased	2.03	8
Cell-to-cell signaling and interaction, cellular movement, hematological system dev. and function, immune cell trafficking	Attraction of monocytes	Increased	2.00	4
Cell death and survival	Apoptosis of leukocytes	Decreased	− 2.63	11

Table 6 Significant upstream regulators identified following IPA upstream analysis of differential gene expression in follicular cells ($P < 0.05$, z score > 2.0)

Upstream regulator	Relative change	Predicted activation state	Activation *z* score	Molecule type
AGT	1.73	Activated	2.926	Growth factor
EGF	1.12	Activated	2.759	Growth factor
IL6	1.38	Activated	2.578	Cytokine
IL1B	1.79	Activated	2.542	Cytokine
Tnf (family)		Activated	2.403	Group
ERK1/2		Activated	2.401	Group
MAP3K8	1.19	Activated	2.400	Kinase
PDGF BB		Activated	2.394	Complex
EGFR	− 1.22	Activated	2.380	Kinase
TREM1	1.14	Activated	2.377	Trans-membrane receptor
ERK		Activated	2.364	Group
IL17A	− 1.12	Activated	2.336	Cytokine
IKBKB	− 1.26	Activated	2.254	Kinase
NFkB (complex)		Activated	2.251	Complex
SELPLG	1.21	Activated	2.236	Other
CD14	1.01	Activated	2.231	Trans-membrane receptor
Leukotriene D4		Activated	2.230	Chemical-endo. mammalian
IL12 (complex)		Activated	2.226	Complex
GSK3B	− 1.26	Activated	2.216	Kinase
E. coli lipopolysaccharide		Activated	2.215	Chemical-endo. non-mammalian
EGR1	1.54	Activated	2.215	Transcription regulator
IFI16	1.24	Activated	2.213	Transcription regulator
CD40	− 1.25	Activated	2.203	Trans-membrane receptor
JUN	1.17	Activated	2.202	Transcription regulator
AIMP1	1.17	Activated	2.200	Cytokine
KITLG	1.27	Activated	2.195	Growth factor
Fcer1		Activated	2.191	Complex
IL1A	− 1.38	Activated	2.181	Cytokine
CCL5	− 1.08	Activated	2.180	Cytokine
Tlr		Activated	2.173	Group

Table 6 (continued)

Upstream regulator	Relative change	Predicted activation state	Activation *z* score	Molecule type
MYD88	− 1.08	Activated	2.155	Other
Estrogen		Activated	2.076	Chemical drug
STAT3	− 1.23	Activated	2.065	Transcription regulator
TLR3	1.25	Activated	2.030	Trans-membrane receptor
HIF1A	1.45	Activated	2.019	Transcription regulator
Mapk		Activated	2.000	Group
NPM1	− 1.23	Inhibited	− 2.000	Transcription regulator
IL10RA	− 1.03	Inhibited	− 2.000	Trans-membrane receptor
FOSL1	− 1.18	Inhibited	− 2.137	Transcription regulator
SFTPA1	− 1.04	Inhibited	− 2.184	Transporter
Diphenyleneiodonium		Inhibited	− 2.236	Chemical reagent (ROS inhibitor)

PTMA) were analyzed by quantitative RT-PCR (Fig. 2). The microarray analysis previously showed that *CXCL2, DOK5, IL1B, IL8*, and *NTS* were overexpressed in the negative group compared to the positive group, while *PTMA* was under-expressed. When looking at the 32 patients that were used in the microarray analysis, the qRT-PCR results are consistent with those of the microarray. All genes are in the expected direction, with *CXCL2* and *DOK5* reaching significance and *NTS* having a *P* value of 0.06 (Fig. 2a). Moreover, it is interesting to note that when all samples from negative ($n = 28$) and positive ($n = 69$) groups were individually analyzed by qRT-PCR, expression of *DOK5* and *NTS* was still significantly higher in the negative group (Fig. 2b). Finally, there was no difference between positive and negative samples regarding the expression level of *CD45* (*P* value = 0.4804).

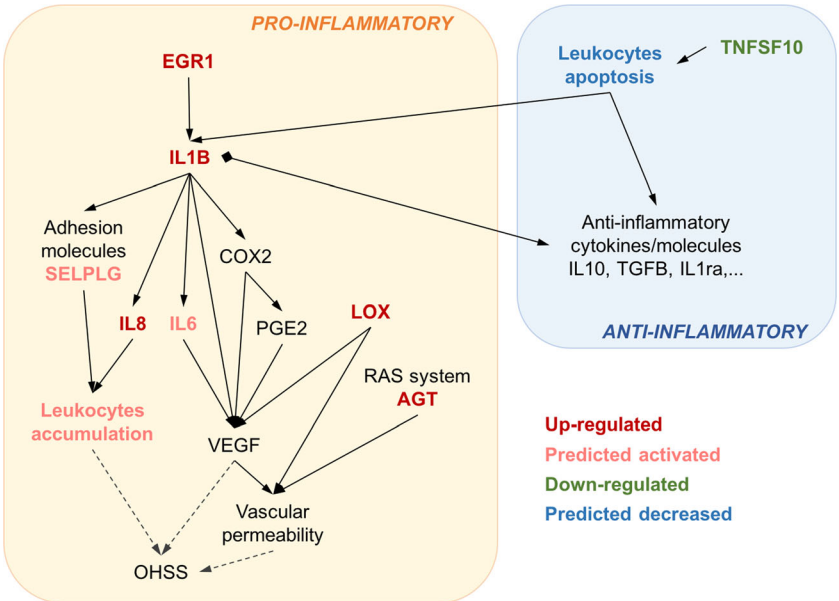

Fig. 1 Schematic illustration of the principal differentially expressed genes and upstream regulators identified in the study and their interactions with each other in the inflammatory response. Items in the left orange box are known to be pro-inflammatory whereas those in the blue box are known to be anti-inflammatory. Red gene or function indicates upregulation, green indicates downregulation, pink indicates predicted activation, and blue indicates predicted decrease (always in the negative group compared to the successful IVF group). *EGR1*: early growth response 1; *IL1B*: interleukin 1 beta; *SELPLG*: selectin P ligand; *IL8*: interleukin 8; *IL6*: interleukin 6; *COX2*: cyclooxygenase 2; *PGE2*: prostaglandin E2; *LOX*: lysyl oxidase; *AGT*: angiotensinogen; *VEGF*: vascular endothelial growth factor; OHSS: ovarian hyperstimulation syndrome; *TNFSF10*: tumor necrosis factor superfamily member 10; *IL10*: interleukin 10; *TGFB*: transforming growth factor beta; *IL1ra*: interleukin 1 receptor antagonist

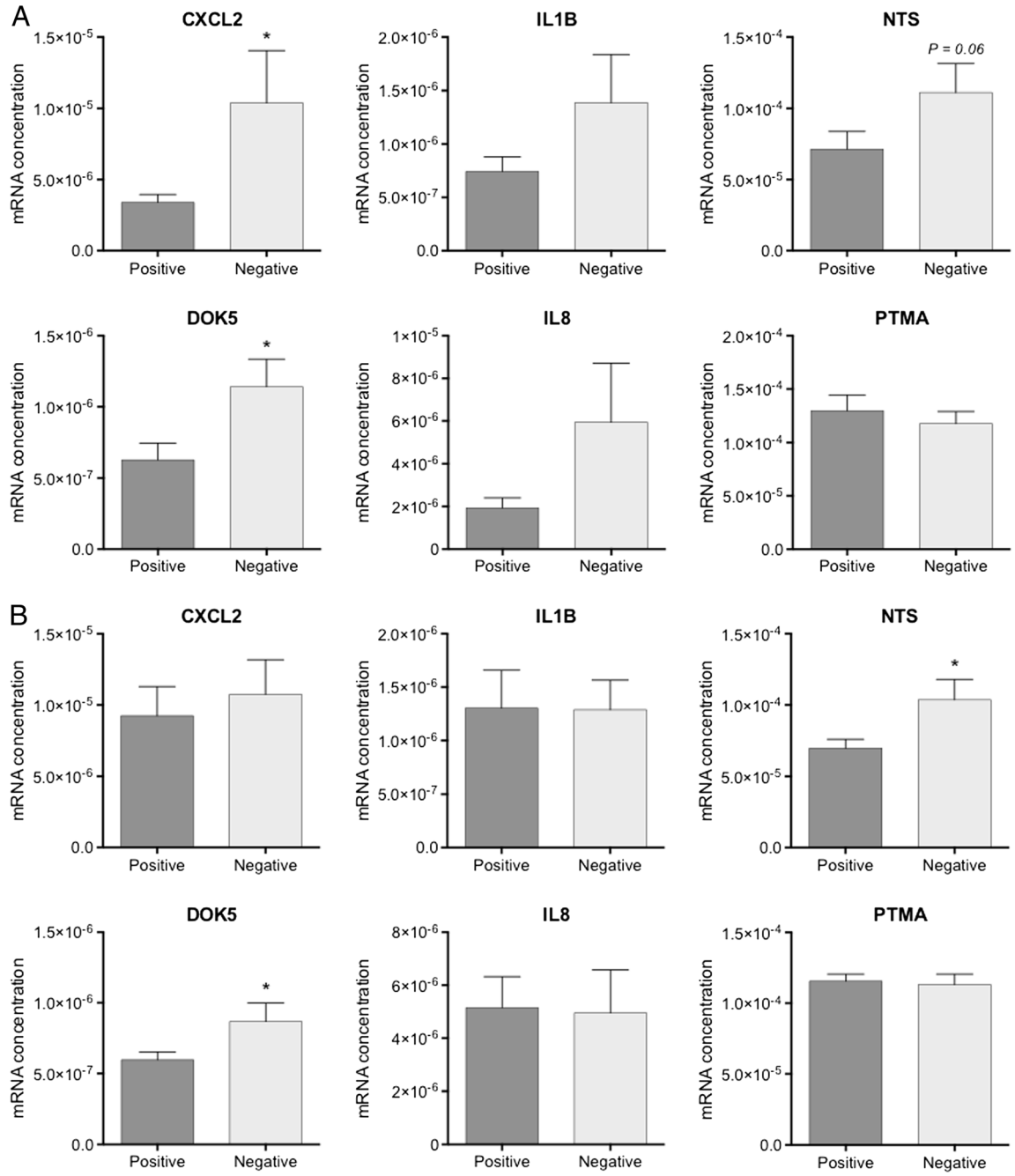

Fig. 2 Quantitative RT-PCR analysis of chemokine C-X-C motif ligand 2 (*CXCL2*), docking protein 5 (*DOK5*), interleukin 8 (*IL8*), interleukin 1 beta (*IL1B*), neurotensin (*NTS*), and prothymosin alpha (*PTMA*) in the failed IVF group compared to the positive group. **a** Quantitative RT-PCR of negative ($n = 16$) and positive ($n = 16$) patients used in the microarray. An asterisk indicates a significant difference ($P < 0.05$) following t test. Data are mean ± SEM. Data were log transformed to meet criteria for normality before performing the t test, but graphics are presented with non-transformed data. **b** Quantitative RT-PCR of all patients from negative ($n = 28$) and positive ($n = 69$) groups. An asterisk indicates a significant difference ($P < 0.05$) between the positive and negative groups following Mann-Whitney test. Data are mean ± SEM

Discussion

In this study, gene expression in ovarian follicular cells obtained from patients undergoing IVF treatment for infertility was analyzed using a microarray covering the human transcriptome. This is the first time that a pool of all follicles from a given cycle are used to explore failure. The study design was set to uncover common differences in a group of 32 patients thus minimizing genetic differences or treatment differences. Patients that did not become pregnant following the IVF cycle were compared to those that did. A total of 165 genes were differentially expressed, with fold-changes ranging from 2.47 to − 2.33, showing different gene expression profiles in patients with a failed cycle.

As shown in Table 1, negative and positive patients did not seem to be different, which confirms the difficulty of assessing failure to simple indicators like follicle number or estradiol level.

Six genes differentially expressed in the microarray were analyzed by qRT-PCR in the 32 patients from the array and the results were consistent with both techniques (Fig. 2a). The validation was also performed in an enlarged cohort (Fig. 2b). Only two of the six genes reached significance, but this is not very surprising considering that qPCR and microarray are two completely different approaches with two completely different goals. The whole transcriptome microarray is a global investigating approach; it provides a big picture, analyzing more than 40,000 probes at the same time. The microarray is particularly advantageous when changes in individual genes are of moderate amplitude, since group effects can be revealed using different tools, for example those designed to identify the principal pathways affected or those designed to identify upstream regulators based on changes in several individual downstream targets. Many genes could not be used on their own because of their insufficient significativity, but could become very powerful when used in combination with other genes. Therefore, since qPCR is a single gene approach, if the changes in the individual genes of a microarray experiment are of moderate amplitude (like it is the case here with fold-changes ranging − 2.5 to 2.5), it makes them very difficult to validate.

The results obtained in the present study highlight the importance of the immune system and the inflammatory reactions associated with the ovulation process. Others before have noted the striking molecular similarity between ovulation and the acute inflammatory response [20]. The ovulatory process requires tissue breakdown, as well as tissue remodeling and active angiogenesis to form the highly vascularized corpus luteum [21]. Like in any lesion, a cascade of biochemical events propagates and enhances the pro-inflammatory response, which must be kept under active control by a concurrent anti-inflammatory response to prevent inflammation from becoming excessive and leading to cell destruction. A closely regulated balance between pro-inflammatory genes involved in proteolysis and anti-inflammatory genes involved in maintaining follicle integrity, repairing the traumatized ovary and resorbing inflammation thus ensures the harmonious progression of the ovulatory process [22].

An interesting result emerging from this study is that failure to conceive following ovarian stimulation is associated with an imbalance between pro-inflammatory and anti-inflammatory mediators (Fig. 1). Indeed, many of the differentially expressed genes in this contrast encode pro-inflammatory cytokines or other factors related to inflammation that have been seen transcriptionally active in granulosa cells [23–26]. For example, chemokine C-C motif ligand 3 (*CCL3*), chemokine C-X-C motif ligand 8 (*CXCL8*) or interleukin 8 (*IL8*), chemokine C-X-C motif ligand 2 (*CXCL2*), interleukin 1 beta (*IL1B*) and chemokine C-C motif ligand 4 (*CCL4*) were all upregulated in the negative group compared to the positive group. Along with these, early growth response 1 (*EGR1*), a known master switch in the induction of pro-inflammatory mediators, was also upregulated and identified among the major upstream regulators [27]. *EGR1* is a pro-inflammatory zinc finger transcription factor induced rapidly by various extracellular stimuli [28]. *EGR1* promotes the sustained expression of several genes that are important in inflammation, coagulation, and vascular hyper-permeability [27, 29] and mediates induction of both CC and CXC class chemokines [27], which is consistent with the observed overexpression of *CCL3, IL8, CXCL2*, and *CCL4*. Target genes downstream from *EGR1* also include the upregulated *IL1B* and tumor necrosis factor (*TNF*), which encode the two main cytokines that orchestrate the pro-inflammatory process [30–32]. Cytokines have been studied widely over the past few decades and are now recognized as important intra-ovarian regulators of folliculogenesis, ovulation, and corpus luteum function [33]. However, exaggerated production of pro-inflammatory cytokines or a persistent pro-inflammatory response may result in deterioration rather than restoration of homeostasis [34].

In addition to the sustained pro-inflammatory response, the anti-inflammatory mechanisms normally helping restoration of homeostasis seem to be impaired in the negative group. Counter-regulatory mechanisms normally control the acute phase via concurrent production of anti-inflammatory mediators such as interleukin 10, interleukin 4, transforming growth factor beta (*TGFB*), soluble tumor necrosis factor receptor, or interleukin 1 receptor antagonist (*IL-1ra*), which inactivate pro-inflammatory mediators or downregulate their production [35–37]. Apoptosis of leukocytes is another crucial process in the control and resolution of inflammation, since it suppresses the production of pro-inflammatory factors and induces the release of anti-inflammatory signals such as *IL-10* and *TGFB* [38–40]. However, in the present study, interleukin 10 receptor subunit alpha (*IL-10RA*) was among the few upstream regulators that IPA predicted would be inhibited, and apoptosis of leukocytes was the only biological function that IPA functional analysis predicted would be decreased. Significant downregulation of tumor necrosis factor superfamily member 10 was also observed, and this gene (*TNFSF10*) is known to accelerate apoptosis of leukocytes (Fig. 1) [41, 42]. These results further support the hypothesis that the ovarian environment created by hormonal stimulation is prone to dysregulation and acute inflammation due to the pro-inflammatory response not being shut off in time or modulated by an appropriate anti-inflammatory response.

Our results also suggest increased vascular permeability, vasodilatation, and leukocytosis, which are known to be associated with clinical manifestations of OHSS. None of the patients presented clinical OHSS after the ovarian stimulation. The unbalanced inflammation in our negative group could

therefore reflect an intermediate/abnormal state of response in some patients. OHSS is an exaggerated ovarian response to the development of large numbers of follicles. It is the most serious complication of ovarian stimulation and it illustrates the consequences of excessive response to stimulation and uncontrolled inflammation [43]. It is now generally believed that increased vascular permeability is the primary initial change that leads to the appearance of OHSS-like symptoms and that vascular endothelial growth factor (*VEGF*) is its principal mediator [44–46].

In the present study, overexpression of several factors indicates increased permeability and vasodilation in the negative group and some factors acting upstream from *VEGF* were also overexpressed. Indeed, hypoxia-inducible factor 1-alpha, which is known to induce transcription of *VEGF* [47], was identified among the upstream regulators and tended to be overexpressed. The peptide adrenomedullin is a known potent vasodilator [48, 49] and was also significantly overexpressed in the failed IVF group. Interleukin 1B (also increased significantly in this group and listed among the activated upstream regulators) promotes the expression of *VEGF* and *COX2* [50, 51]. Another factor that was upregulated significantly in the negative group is lysyl oxidase (*LOX*), a copper-dependent amine oxidase that plays a critical role in the formation and repair of the extracellular matrix by cross-linking collagen and elastin [52]. It has been shown that *LOX* promotes *VEGF* secretion in vitro and angiogenesis in live mice (Baker et al. [53]. Deviations from normal extracellular matrix cross-linking and rigidity may result in increased vascular permeability [54]. The overexpression of angiotensinogen (*AGT*) and its predicted activated state as upstream regulator indicates the ovarian renin–angiotensin system (RAS) activation in the failed IVF group. The RAS has been found to be an important factor in increased vascular permeability [55].

Another mechanism that appears more pronounced in the negative group is the recruitment of immune cells to ovarian tissues, which might reflect leukocytosis. As mentioned earlier, *TNFSF10* promotes leukocyte apoptosis and it was downregulated. Moreover, almost all the gene annotations identified by IPA were related to promotion of cell's chemotaxis, movement, mobilization or infiltration, or to increase the counts or recruitment of various immune cells type such as neutrophils, lymphocytes, and macrophages. In addition to its functions already mentioned, *IL-1B* (overexpressed in negative group) promotes the expression or release of adhesion molecules such as p-selectins [56, 57], which is consistent with the presence of the high-affinity counter-receptor for p-selectin (selectin P ligand or *SELPLG*) among the activated upstream regulators. Inflamed endothelial cells express p-selectins in response to inflammatory stimuli (histamine, PAF, IL-1b, TNF). The interaction of these molecules with their ligands leads to rapid attachment of leukocytes to blood vessels [58, 59]. *IL-1B* also induces the release of pro-inflammatory cytokines IL-6 and IL-8 [60]. *IL6* tended to be overexpressed in the negative group (fold-change of 1.38) and was also identified as an upstream regulator (z score of 2.58). It is a known promoter of neutrophil activation and potentiates lymphocyte growth and proliferation in synergism with *IL-1B* and *TNF* [61]. Interleukin 8, which was significantly overexpressed, is a known potent chemoattractant and activator of neutrophils. Following their adhesion to the endothelial cell wall, neutrophils invade inflamed tissue in response to IL-8 and other chemokines [59, 62]. Once in the inflamed tissue, they become an additional source of cytokines, chemokines, and other factors that further intensify the pro-inflammatory loop. Although increases in follicle leukocyte counts at the onset of ovulation and in the regressing corpus luteum are normal [63, 64] and that stimulation with gonadotropin does induce leukocytosis to some degree, it is likely that this latter phenomenon is more pronounced in OHSS patients [65]. As shown by the present study, it could also affect the IVF outcome in non-OHSS patients.

Inflammation is probably not the primary explanation, but rather an indicator that some important aspect of the ovulation process has gone awry. The stimulation itself plus the fact that many follicles are growing could exacerbate inflammation, although this latter effect appears highly variable and might even improve the prognosis, as seen in younger patients or in those with a better ovarian reserve. In a typical menstrual cycle, development of only few follicles and ultimately of a single corpus luteum does not result in OHSS [60]. In contrast, ovarian stimulation leads to the development of additional follicles and corpus luteum and thus to larger amounts of the numerous factors produced by these structures, as the higher levels of cytokines and immune cells in stimulated cycles illustrate [65–67]. Several cytokines are able to induce enzymes that generate reactive oxygen species (ROS) and leukocytes are a major source of ROS as well. Although beneficial at normal levels, ROS are cytotoxic in high doses and often lead to cell damage or cell death [68]. Pleiotropic effects make it clear that inflammatory mediators play an important role in the ovary but also that they have the potential to compromise oocyte quality via numerous mechanisms.

Finally, other differentially expressed genes like uromodulin-like 1 (*UMODL1*) and prothymosin alpha (*PTMA*) are related to abnormal differentiation and increased apoptosis, two phenomena also associated with follicular aging that could also be potential failure causes. *UMODL1* was the most overexpressed gene, while *PTMA* was the most under-expressed gene in the negative group. This gene is located in the minimal region of chromosome 21 and was reported first in association with Down's syndrome and congenital myopia [69–71] and later with accelerated follicle depletion and ovarian degeneration. It is regulated by gonadotropins, and mice carrying extra copies show reduced fertility and elevated apoptosis in growing ovarian follicles and in oocytes [72]. This same study also showed that it could play a role in

crosstalk between the immune and reproductive systems. Its upregulation has been observed in the largest incompetent follicles in patients receiving hormonal treatment for IVF [17], which is consistent with our results. PTMA is an anti-apoptotic factor [73] that acts by blocking the formation of the apoptosome [74, 75]. Significant downregulation of *PTMA* in the negative group might reflect reduced anti-apoptotic activity and hence increased apoptosis.

While inflammation and apoptosis may or may not be linked, either would likely have an impact on oocyte quality, and monitoring them could suggest specific approaches for individual patients. Since we were working with a heterogenous cohort of patient that were pooled according to outcome, it is possible (and expected) that we have at least two or three different causes or levels of failure mixed into our negative population. This would also explain the moderate amplitude of gene expression changes.

The information in relation with the cause of failure can be used to address and customize the stimulation and trigger conditions according to each patient profile. Using specific means to increase follicular synchrony or modify trigger conditions may be applied if the granulosa cells are analyzed with markers of failure causes. In addition to the genes showing up in failure cases, it is clear that some patient may have individual infertility problems, defective receptors, or other genetic anomalies that would not appear in such type of general failure analysis.

Conclusion

Better understanding the reasons for the failure of IVF cycles should lead to improved stimulation protocols and more successful treatment of infertility. This study used a global approach to have a better picture of potential failure causes and potential pathways for further investigation. The follicular response to the stimulation is particular to each patient and the differentially expressed genes showing up in this contrast could be the results of different failure causes mixed together. Some differentially expressed genes appear related to abnormal differentiation and increased apoptosis. However, proper control of inflammation appears to be a key element, since our results indicate an impaired balance between pro- and anti-inflammatory mediators. Increased vascular permeability, vasodilation, and leukocytosis suggest an abnormal response that affects oocytes without leading to systemic problems such as those seen in clinical cases of OHSS. We speculate that recruitment of multiple follicles triggers a massive inflammatory reaction, which can create an excessive pro-inflammatory response in some patients. Although some degree of inflammation is an essential part of the ovulatory cycle, it can easily become detrimental when not properly regulated. Stimulatory protocols personalized according to patient response could improve the chances of later success, and the potential use of anti-inflammatory mediators should be investigated in this subpopulation as a complementary solution to the problem of failure to conceive following IVF.

Acknowledgements The authors thank Isabelle Dufort for her support and assistance in the lab, and Scot Hamilton, Marie-Claude Léveillé, Martin Laforest, and Hanane Lachgar for their involvement in the collection of follicle cell samples.

Authors' roles Fortin, C.: conception and design of the study, sample processing, data acquisition, data analysis and interpretation, drafting the article, approval of the final manuscript.

Leader, A.: data acquisition, critical discussion, reading and approval of the final manuscript.

Mahutte, N.: data acquisition, critical discussion, reading and approval of the final manuscript.

Hamilton, S.: data acquisition, critical discussion, reading and approval of the final manuscript.

Léveillé, M.C.: data acquisition, critical discussion, reading and approval of the final manuscript.

Villeneuve, M.: data acquisition, critical discussion, reading and approval of the final manuscript.

Sirard, M.A.: conception and design of the study, data analysis and interpretation, improvement of the draft, reading and approval of the final manuscript.

Funding This work was supported by the Merck Serono Grant for Fertility Innovation (GFI).

Compliance with ethical standards

Conflict of interest The authors declare that they have no conflict of interest. A GFI grant was received in support of this work. This article does not contain any data or conclusion relating to any commercial product.

Ethical approval This project was approved by Université Laval REB (2014-102/08-09-2014) for the collection and use of human tissues.

Large-scale data The data discussed in this publication are accessible through GEO Series accession number GSE87545.

References

1. Canadian Fertility and Andrology Society. Canadian ART Report. Human Assisted Reproduction 2014 Live Birth Rates for Canada 2014.
2. The European IVF-Monitoring Consortium for the European Society of Human Reproduction and Embryology, Calhaz-Jorge C, de Geyter C, Kupka MS, de Mouzon J, Erb K, et al. Assisted reproductive technology in Europe, 2012: results generated from European registers by ESHRE. Hum Reprod. 2016;31(8):1638–52. https://doi.org/10.1093/humrep/dew151.
3. Eppig JJ. Oocyte control of ovarian follicular development and function in mammals. Reproduction. 2001;122(6):829–38.
4. Matzuk MM, Burns KH, Viveiros MM, Eppig JJ. Intercellular communication in the mammalian ovary: oocytes carry the conversation. Science. 2002;296(5576):2178–80. https://doi.org/10.1126/science.1071965.
5. Hamel M, Dufort I, Robert C, Gravel C, Leveille M-C, Leader A, et al. Identification of differentially expressed markers in human

follicular cells associated with competent oocytes. Hum Reprod. 2008;23(5):1118–27. https://doi.org/10.1093/humrep/den048.
6. Hamel M, Dufort I, Robert C, Léveillé M-C, Leader A, Sirard M-A. Genomic assessment of follicular marker genes as pregnancy predictors for human IVF. Mol Hum Reprod. 2010;16(2):87–96. https://doi.org/10.1093/molehr/gap079.
7. Hamel M, Dufort I, Robert C, Léveillé M-C, Leader A, Sirard M-A. Identification of follicular marker genes as pregnancy predictors for human IVF: new evidence for the involvement of luteinization process. Mol Hum Reprod. 2010;16(8):548–56. https://doi.org/10.1093/molehr/gaq051.
8. Uyar A, Torrealday S, Seli E. Cumulus and granulosa cell markers of oocyte and embryo quality. Fertil Steril. 2013;99(4):979–97. https://doi.org/10.1016/j.fertnstert.2013.01.129.
9. Burnik Papler T, Vrtacnik Bokal E, Maver A, Lovrecic L. Specific gene expression differences in cumulus cells as potential biomarkers of pregnancy. Reprod BioMed Online. 2015;30:426–33. https://doi.org/10.1016/j.rbmo.2014.12.011.
10. Gebhardt KM, Feil DK, Dunning KR, Lane M, Russell DL. Human cumulus cell gene expression as a biomarker of pregnancy outcome after single embryo transfer. Fertil Steril. 2011;96(1):47–52 e2. https://doi.org/10.1016/j.fertnstert.2011.04.033.
11. Iager AE, Kocabas AM, Otu HH, Ruppel P, Langerveld A, Schnarr P, et al. Identification of a novel gene set in human cumulus cells predictive of an oocyte's pregnancy potential. Fertil Steril. 2013;99(3):745–52 e6. https://doi.org/10.1016/j.fertnstert.2012.10.041.
12. Wathlet S, Adriaenssens T, Segers I, Verheyen G, Van Landuyt L, Coucke W, et al. Pregnancy prediction in single embryo transfer cycles after ICSI using QPCR: validation in oocytes from the same cohort. PLoS One. 2013;8(4):e54226. https://doi.org/10.1371/journal.pone.0054226.
13. Anderson RA, Sciorio R, Kinnell H, Bayne RA, Thong KJ, de Sousa PA, et al. Cumulus gene expression as a predictor of human oocyte fertilisation, embryo development and competence to establish a pregnancy. Reproduction. 2009;138(4):629–37. https://doi.org/10.1530/REP-09-0144.
14. Assidi M, Montag M, Van der Ven K, Sirard MA. Biomarkers of human oocyte developmental competence expressed in cumulus cells before ICSI: a preliminary study. J Assist Reprod Genet. 2011;28(2):173–88. https://doi.org/10.1007/s10815-010-9491-7.
15. Assou S, Haouzi D, Mahmoud K, Aouacheria A, Guillemin Y, Pantesco V, et al. A non-invasive test for assessing embryo potential by gene expression profiles of human cumulus cells: a proof of concept study. Mol Hum Reprod. 2008;14(12):711–9. https://doi.org/10.1093/molehr/gan067.
16. Feuerstein P, Puard V, Chevalier C, Teusan R, Cadoret V, Guerif F, et al. Genomic assessment of human cumulus cell marker genes as predictors of oocyte developmental competence: impact of various experimental factors. PLoS One. 2012;7(7):e40449. https://doi.org/10.1371/journal.pone.0040449.
17. Nivet AL, Leveille MC, Leader A, Sirard MA. Transcriptional characteristics of different sized follicles in relation to embryo transferability: potential role of hepatocyte growth factor signalling. Mol Hum Reprod. 2016;22:475–84. https://doi.org/10.1093/molehr/gaw029.
18. Blazejczyk M, Miron M, Nadon R. FlexArray: a statistical data analysis software for gene expression microarrays. Montreal, Canada: Genome Quebec 2007.
19. Vandesompele J, De Preter K, Pattyn F, Poppe B, Van Roy N, De Paepe A, et al. Accurate normalization of real-time quantitative RT-PCR data by geometric averaging of multiple internal control genes. Genome Biol. 2002;3(7):RESEARCH0034.
20. Espey LL. Ovulation as an inflammatory reaction—a hypothesis. Biol Reprod. 1980;22(1):73–106.
21. Espey LL, Lipner H. Ovulation. In: Knobil E, Neill JD, editors. The physiology of reproduction. 1 ed. New-York, United-States.: Raven Press; 1994. p. 725–80.
22. Espey LL, Bellinger AS, Healy JA. Ovulation: an inflammatory cascade of gene expression. In: Leung PCK, Adashi EY, editors. The ovary. 2 ed. San Diego, CA, United States: Elsevier Academic Press; 2004. p. 145–165.
23. Adams J, Liu Z, Ren YA, Wun WS, Zhou W, Kenigsberg S, et al. Enhanced inflammatory transcriptome in the granulosa cells of women with polycystic ovarian syndrome. J Clin Endocrinol Metab. 2016;101(9):3459–68. https://doi.org/10.1210/jc.2015-4275.
24. Dahm-Kahler P, Runesson E, Lind AK, Brannstrom M. Monocyte chemotactic protein-1 in the follicle of the menstrual and IVF cycle. Mol Hum Reprod. 2006;12(1):1–6. https://doi.org/10.1093/molehr/gah256.
25. Carletti MZ, Christenson LK. Rapid effects of LH on gene expression in the mural granulosa cells of mouse periovulatory follicles. Reproduction. 2009;137(5):843–55. https://doi.org/10.1530/REP-08-0457.
26. Kaur S, Archer KJ, Devi MG, Kriplani A, Strauss JF 3rd, Singh R. Differential gene expression in granulosa cells from polycystic ovary syndrome patients with and without insulin resistance: identification of susceptibility gene sets through network analysis. J Clin Endocrinol Metab. 2012;97(10):E2016–21. https://doi.org/10.1210/jc.2011-3441.
27. Yan SF, Fujita T, Lu J, Okada K, Shan Zou Y, Mackman N, et al. Egr-1, a master switch coordinating upregulation of divergent gene families underlying ischemic stress. Nat Med. 2000;6(12):1355–61. https://doi.org/10.1038/82168.
28. Beckmann AM, Wilce PA. Egr transcription factors in the nervous system. Neurochem Int. 1997;31(4):477–510 discussion 7-6.
29. Khachigian LM, Collins T. Early growth response factor 1: a pleiotropic mediator of inducible gene expression. J Mol Med (Berl). 1998;76(9):613–6.
30. Cavaillon JM. Cytokines in inflammation. C R Seances Soc Biol Fil. 1995;189(4):531–44.
31. Okada M, Fujita T, Sakaguchi T, Olson KE, Collins T, Stern DM, et al. Extinguishing Egr-1-dependent inflammatory and thrombotic cascades after lung transplantation. FASEB J. 2001;15(14):2757–9. https://doi.org/10.1096/fj.01-0490fje.
32. Silverman ES, De Sanctis GT, Boyce J, Maclean JA, Jiao A, Green FH, et al. The transcription factor early growth-response factor 1 modulates tumor necrosis factor-alpha, immunoglobulin E, and airway responsiveness in mice. Am J Respir Crit Care Med. 2001;163(3 Pt 1):778–85. https://doi.org/10.1164/ajrccm.163.3.2003123.
33. Brannstrom M. Potential role of cytokines in ovarian physiology: the case for interleukin-1. In: Leung PCK, Adashi EY, editors. The ovary. 2 ed. San Diego, CA, United States: Elsevier Academic Press; 2004. p. 261–271.
34. Guirao X, Lowry SF. Biologic control of injury and inflammation: much more than too little or too late. World J Surg. 1996;20(4):437–46.
35. Cassatella MA, Meda L, Bonora S, Ceska M, Constantin G. Interleukin 10 (IL-10) inhibits the release of proinflammatory cytokines from human polymorphonuclear leukocytes. Evidence for an autocrine role of tumor necrosis factor and IL-1 beta in mediating the production of IL-8 triggered by lipopolysaccharide. J Exp Med. 1993;178(6):2207–11.
36. Medzhitov R. Inflammation 2010: new adventures of an old flame. Cell. 2010;140(6):771–6. https://doi.org/10.1016/j.cell.2010.03.006.
37. Muszynski JA, Frazier WJ, Hall MW. Pro-inflammatory and anti-inflammatory mediators in critical illness and injury. In: Wheeler SD, Wong RH, Shanley PT, editors. Pediatric critical care medicine:

volume 1: care of the critically ill or injured child. London: Springer London; 2014. p. 231–8.
38. Haslett C. Granulocyte apoptosis and inflammatory disease. Br Med Bull. 1997;53(3):669–83.
39. Huynh ML, Fadok VA, Henson PM. Phosphatidylserine-dependent ingestion of apoptotic cells promotes TGF-beta1 secretion and the resolution of inflammation. J Clin Invest. 2002;109(1):41–50. https://doi.org/10.1172/JCI11638.
40. Voll RE, Herrmann M, Roth EA, Stach C, Kalden JR, Girkontaite I. Immunosuppressive effects of apoptotic cells. Nature. 1997;390(6658):350–1. https://doi.org/10.1038/37022.
41. McGrath EE, Marriott HM, Lawrie A, Francis SE, Sabroe I, Renshaw SA, et al. TNF-related apoptosis-inducing ligand (TRAIL) regulates inflammatory neutrophil apoptosis and enhances resolution of inflammation. J Leukoc Biol. 2011;90(5):855–65. https://doi.org/10.1189/jlb.0211062.
42. Renshaw SA, Parmar JS, Singleton V, Rowe SJ, Dockrell DH, Dower SK, et al. Acceleration of human neutrophil apoptosis by TRAIL. J Immunol. 2003;170(2):1027–33.
43. Bergh PA, Navot D. Ovarian hyperstimulation syndrome: a review of pathophysiology. J Assist Reprod Genet. 1992;9(5):429–38.
44. McClure N, Healy DL, Rogers PA, Sullivan J, Beaton L, Haning RV Jr, et al. Vascular endothelial growth factor as capillary permeability agent in ovarian hyperstimulation syndrome. Lancet. 1994;344(8917):235–6.
45. Soares SR, Gomez R, Simon C, Garcia-Velasco JA, Pellicer A. Targeting the vascular endothelial growth factor system to prevent ovarian hyperstimulation syndrome. Hum Reprod Update. 2008;14(4):321–33. https://doi.org/10.1093/humupd/dmn008.
46. Vlahos NF, Gregoriou O. Prevention and management of ovarian hyperstimulation syndrome. Ann N Y Acad Sci. 2006;1092:247–64. https://doi.org/10.1196/annals.1365.021.
47. Lee JW, Bae SH, Jeong JW, Kim SH, Kim KW. Hypoxia-inducible factor (HIF-1)alpha: its protein stability and biological functions. Exp Mol Med. 2004;36(1):1–12. https://doi.org/10.1038/emm.2004.1.
48. Kim W, Moon SO, Sung MJ, Kim SH, Lee S, So JN, et al. Angiogenic role of adrenomedullin through activation of Akt, mitogen-activated protein kinase, and focal adhesion kinase in endothelial cells. FASEB J. 2003;17(13):1937–9. https://doi.org/10.1096/fj.02-1209fje.
49. Sugo S, Minamino N, Shoji H, Kangawa K, Kitamura K, Eto T, et al. Interleukin-1, tumor necrosis factor and lipopolysaccharide additively stimulate production of adrenomedullin in vascular smooth muscle cells. Biochem Biophys Res Commun. 1995;207(1):25–32. https://doi.org/10.1006/bbrc.1995.1148.
50. Ando M, Kol S, Kokia E, Ruutiainen-Altman K, Sirois J, Rohan RM, et al. Rat ovarian prostaglandin endoperoxide synthase-1 and -2: periovulatory expression of granulosa cell-based interleukin-1-dependent enzymes. Endocrinology. 1998;139(5):2501–8. https://doi.org/10.1210/endo.139.5.5988.
51. Levitas E, Chamoun D, Udoff LC, Ando M, Resnick CE, Adashi EY. Periovulatory and interleukin-1 beta-dependent up-regulation of intraovarian vascular endothelial growth factor (VEGF) in the rat: potential role for VEGF in the promotion of periovulatory angiogenesis and vascular permeability. J Soc Gynecol Investig. 2000;7(1):51–60.
52. Smith-Mungo LI, Kagan HM. Lysyl oxidase: properties, regulation and multiple functions in biology. Matrix Biol. 1998;16(7):387–98.
53. Baker AM, Bird D, Welti JC, Gourlaouen M, Lang G, Murray GI, et al. Lysyl oxidase plays a critical role in endothelial cell stimulation to drive tumor angiogenesis. Cancer Res. 2013;73(2):583–94. https://doi.org/10.1158/0008-5472.CAN-12-2447.
54. Mammoto A, Mammoto T, Kanapathipillai M, Wing Yung C, Jiang E, Jiang A, et al. Control of lung vascular permeability and endotoxin-induced pulmonary oedema by changes in extracellular matrix mechanics. Nat Commun. 2013;4:1759. https://doi.org/10.1038/ncomms2774.
55. Vloeberghs V, Peeraer K, Pexsters A, D'Hooghe T. Ovarian hyperstimulation syndrome and complications of ART. Best Pract Res Clin Obstet Gynaecol. 2009;23(5):691–709. https://doi.org/10.1016/j.bpobgyn.2009.02.006.
56. Bevilacqua MP, Pober JS, Wheeler ME, Cotran RS, Gimbrone MA Jr. Interleukin-1 activation of vascular endothelium. Effects on procoagulant activity and leukocyte adhesion. Am J Pathol. 1985;121(3):394–403.
57. Bevilacqua MP, Pober JS, Wheeler ME, Cotran RS, Gimbrone MA Jr. Interleukin 1 acts on cultured human vascular endothelium to increase the adhesion of polymorphonuclear leukocytes, monocytes, and related leukocyte cell lines. J Clin Invest. 1985;76(5):2003–11. https://doi.org/10.1172/JCI112200.
58. Ley K, Laudanna C, Cybulsky MI, Nourshargh S. Getting to the site of inflammation: the leukocyte adhesion cascade updated. Nat Rev Immunol. 2007;7(9):678–89. https://doi.org/10.1038/nri2156.
59. Nourshargh S, Alon R. Leukocyte migration into inflamed tissues. Immunity. 2014;41(5):694–707. https://doi.org/10.1016/j.immuni.2014.10.008.
60. Rizk B, Aboulghar M, Smitz J, Ron-El R. The role of vascular endothelial growth factor and interleukins in the pathogenesis of severe ovarian hyperstimulation syndrome. Hum Reprod Update. 1997;3(3):255–66.
61. Wong GG, Clark SC. Multiple actions of interleukin 6 within a cytokine network. Immunol Today. 1988;9(5):137–9. https://doi.org/10.1016/0167-5699(88)91200-5.
62. Hammond ME, Lapointe GR, Feucht PH, Hilt S, Gallegos CA, Gordon CA, et al. IL-8 induces neutrophil chemotaxis predominantly via type I IL-8 receptors. J Immunol. 1995;155(3):1428–33.
63. Brannstrom M, Pascoe V, Norman RJ, McClure N. Localization of leukocyte subsets in the follicle wall and in the corpus luteum throughout the human menstrual cycle. Fertil Steril. 1994;61(3):488–95.
64. Norman R, Bonello N, Jasper M, Van der Hoek K. Leukocytes: essential cells in ovarian function and ovulation. Reprod Med Rev. 1997;6(02):97–111. https://doi.org/10.1017/S0962279900001447.
65. Hock DL, Huhn RD, Kemmann E. Leukocytosis in response to exogenous gonadotrophin stimulation. Hum Reprod. 1997;12(10):2143–6.
66. Fabregues F, Balasch J, Manau D, Jimenez W, Arroyo V, Creus M, et al. Haematocrit, leukocyte and platelet counts and the severity of the ovarian hyperstimulation syndrome. Hum Reprod. 1998;13(9):2406–10.
67. Loret de Mola JR, Baumgardner GP, Goldfarb JM, Friedlander MA. Ovarian hyperstimulation syndrome: pre-ovulatory serum concentrations of interleukin-6, interleukin-1 receptor antagonist and tumour necrosis factor-alpha cannot predict its occurrence. Hum Reprod. 1996;11(7):1377–80.
68. Bertout JA, Mahutte NG, Preston SL, Behrman HR. Reactive oxygen species and ovarian function. In: Leung PCK, Adashi EY, editors. The ovary. 2 ed. San Diego, CA, United States: Elsevier Academic Press; 2004. p. 353–368.
69. Davisson MT, Bechtel LJ, Akeson EC, Fortna A, Slavov D, Gardiner K. Evolutionary breakpoints on human chromosome 21. Genomics. 2001;78(1–2):99–106. https://doi.org/10.1006/geno.2001.6639.
70. Nishizaki R, Ota M, Inoko H, Meguro A, Shiota T, Okada E, et al. New susceptibility locus for high myopia is linked to the uromodulin-like 1 (UMODL1) gene region on chromosome 21q22.3. Eye (Lond). 2009;23(1):222–9. https://doi.org/10.1038/eye.2008.152.
71. Shibuya K, Nagamine K, Okui M, Ohsawa Y, Asakawa S, Minoshima S, et al. Initial characterization of an uromodulin-like 1 gene on human chromosome 21q22.3. Biochem Biophys Res

Commun. 2004;319(4):1181–9. https://doi.org/10.1016/j.bbrc.2004.05.094.

72. Wang W, Tang Y, Ni L, Kim E, Jongwutiwes T, Hourvitz A, et al. Overexpression of uromodulin-like1 accelerates follicle depletion and subsequent ovarian degeneration. Cell Death Dis. 2012;3:e433. https://doi.org/10.1038/cddis.2012.169.
73. Rodriguez P, Vinuela JE, Alvarez-Fernandez L, Gomez-Marquez J. Prothymosin alpha antisense oligonucleotides induce apoptosis in HL-60 cells. Cell Death Differ. 1999;6(1):3–5. https://doi.org/10.1038/sj.cdd.4400450.
74. Jiang X, Kim HE, Shu H, Zhao Y, Zhang H, Kofron J, et al. Distinctive roles of PHAP proteins and prothymosin-alpha in a death regulatory pathway. Science. 2003;299(5604):223–6. https://doi.org/10.1126/science.1076807.
75. Qi X, Wang L, Du F. Novel small molecules relieve prothymosin alpha-mediated inhibition of apoptosome formation by blocking its interaction with Apaf-1. Biochemistry. 2010;49(9):1923–30. https://doi.org/10.1021/bi9022329.